Kufa Journal of Engineering
Vol. 16, No. 4, October 2025, P.P. 405-418
Article history: Received 19 September 2024, last revised 19 December 2024, accepted 16 February 2025

MICROSTRUCTURE AND MECHANICAL BEHAVIOR OF AISI 1018 DUAL PHASE STEEL PRODUCED VIA INTER-CRITICAL HEAT TREATMENT

Suaad M. Jiaad[1] and Khansaa D. Salman[2]

[1] Department of Electromechanical Engineering, University of Technology, Baghdad, Iraq. Email: 50181@uotechnology.edu.iq.

[2] Department of Aeronautical Techniques Engineering, Bilad Alrafidain University College, Diyala, Iraq. Email: dr.khansaa@bauc14.edu.iq

https://doi.org/10.30572/2018/KJE/160423

ABSTRACT

In the present work, the effect of inter-critical heating temperatures on the micro-structure, microhardness, and wear properties of AISI 1018 steel has been investigated. AISI 1018 steel was heated at three different temperatures 750°C, 775°C, and 800°C inter-critical temperatures for 30 min and followed by hardening in salt water. The results of this study showed that the concentration of martensite phase increases by incrementing inter-critical temperature as 36% Vm. till 70% Vm. At 750°C and 775°C there is one-stage of work hardening has taken place, while two stage have taken place at 800°C. The exponent of work hardening (n) increases with increments of temperature by 0.239 at 750°C, 0.302 at 775°C, and 0.391 at 800°C. While the mechanical properties, such as microhardness, yielding strength, and tension strength have been increased by 162 (HV), 599 MPa and 800 MPa respectively, with an increment of the concentration of the martensite phase till 50%, at which the concentration of the martensite phase is equal to the concentration of the ferrite phase and then slightly increases. Finally, the results of wear behavior reveal that the rate of wear decreases with increasing the temperature of heat treatment by 60×10-7 to 30×10-7, as shown in Fig.9. The photomicrographs of worn surfaces have shown that the grooves of the sample heated at 800°Care finer than for the samples heated at 750°C and 775°C owing to the increase in the concentration of the martensite phase.

KEYWORDS

Inter-critical heating treatment, AISI 1018 carbon steel, microstructure, hardness, wear.

1. INTRODUCTION

Advanced high strength steel (AHSS) has many industrial applications owing to its properties such as light weight, good forming, and high strength. Nowadays, large efforts were made to improve special steel used in automotive industries. To minimize the energy losses, it is necessary to use light weight alloys with high strength. For this reason, special steel with high strength has been produced. The special steel with high strength includes complex steel, martensitic steel, transformation base plasticity steel, twinning base plasticity steel, dual-phase steel and shear band strength steel, aluminum introduced into low weight steel with so much plasticity (Papa Rao, M, et al. 2014; Lai, Q., Bouaziz, et al. 2015; Hug, E., et al. 2015). On the other side, dual-phase steel is cheap and easy to form compared with other categories of special steels. Special steel with high strength has good formability and high strength which enables them to be used in automotive industry applications for many parts of automobiles and bumpers. The main characteristics of dual-phase steel are good elongation, high strength, a low yielding strength to tension strength ratio with good exponent work hardening, a homogeneous microstructure, good weldability and good thermal stability. Dual-phase steel generally has a hard phase (martensite) and a ductile phase (ferrite) as a matrix. These phases give the dual-phase steel high strength and good ductility (Hertzberg, R. W., et al. 2020). Recently, inter-critical heat treatments have been used to improve dual-phase steel to obtain special strength and good ductility for low-carbon steel containing carbon elements less than 0.2 % C. Dual-phase steel consists of two phases, one of them is the ductile phase (ferrite) and the other is the hard phase (martensite), which precipitates at the grain boundaries of ferrite with a little amount of the bainite phase. To obtain these phases, the steel is heated in the inter-critical region ($\alpha+\gamma$) which is between the lower inter-critical temperature (A1) and the high inter-critical temperature (A3) followed by quenching in a suitable quenching medium (Hug, E., Martinez, et al. 2016). Dual-phase steel is important for vehicle industries without needing a forming process while needing low cost. Through the inter-critical heat treatment in the ($\alpha+\gamma$) region, the austenite phase will transform to the martensite phase and create a few dislocations in the α matrix. Plastic deformation which in turn minimizes yielding stress and increases tensile strength and ductility (Pandre, S., Takalkar, et al. 2020). On the other hand, the plastic deformation an increase with an increase in the content of the hard phase (martensite). The optimum values of ductility and tensile strength are obtained at equal amounts of concentration of the ferrite phase and martensite phase (equal to 50%). Moreover, increasing the tensile strength leads to decrease the toughness especially at low temperatures. The inter-critical heat treatment is a good process to produce dual-phase steel microstructure containing ferrite and

martensite phases to obtain high tensile strength and toughness which it is difficult to obtain by conventional heat treatment. Nowadays, the inter-critical heat treatment of steel consists of 4-10 wt.% manganese element that has been used to produce ferrite-austenite steel. However, this steel is more expensive and difficult for welding. For steel contains low carbon element less than 0.1 wt.% manganese element must be low than 2-3 wt.% to make it more economical. To make the retained austenite stable with high tensile strength in dual-phase steel and high toughness in low carbon low alloy steel, the inter-critical heat treatment must be done in two stages (Jiang, J., Wu, et al. 2013). Dual-phase steels are utilized in pressure vessels, structural parts, pipelines, gas pipelines and ship hulls owing to their high strength, good ductility, high toughness, low yield strength and good weldability (Pervaiz, S., et al. 2016; Ebrahimian, A., et al. 2017). The high strength, low yielding strength, good plasticity and formability with good work hardening can be obtained by a uniform dispersion of hard phase (martensite) into ductile phase (ferrite). Commonly dual-phase steel can be produced by inter-critical heat treatment in the ($\alpha+\gamma$) region followed by quenching heat treatment. During quenching heat treatments, the austenitic phase will transforms to martensite phase, while the ferrite phase transform and then produces ductile-phase steel. The microstructural analysis of the produced dual-phase consists of the martensite phase (M) dispersed into the ferrite phase (α) instead of the original phases at room temperature the ferrite phase (α) and the pearlite phase (P) (Ebrahimian, A., et al. 2017). The morphology of the dispersion of martensite phase into ferrite phase shows exceptional properties of dual-phase steel such as high strength and high toughness with good ductility. The transformation mechanism of the austenitic phase to the martensitic phase (M) discussed as follows: During the transformation of the austenitic phase to the martensitic phase creates a network of line defects into ferrite phase. The movement of line defects (dislocations) causes plastic flow which in turn causes plastic strain. The plastic flow creates a low yielding point and gives low yield stress (Namdev, A., et al. 2022). In the recent decades, many efforts have been done to develop dual-phase steel for vehicle industries owing to reducing the weight of vehicles and increasing the usage of dual-phase steel in automotive industries. Owing to the exceptional features of the microstructure of dual-phase steel, the martensite phase creates a ferrite phase enabling this type of steel to be used in vehicle industries. In vehicle industries, the carbon element is deeply affected by the forming and welding properties, increasing the carbon percent will extremely affected on the amount of martensite and cause inverse properties. Recently, many researchers have been done for another type of steel containing more than 0.3 wt.% C to improve the wear properties of dual-phase steel (Shukla, N., et al. 2016; Deng, Y., et al. 2019).

(Abbas K. Hussein et al. 2018) have been studied the preferred parameters for the heat treatment (temperature and time of quenching and tempering, type of nanoparticle and its weight percentage) to increase the microhardness of medium carbon steel by the Taguchi technique. While (Sundus A. Shukur and Hayder H. Al Khudery 2023) have been studied the mechanical properties and bonding strength of steel fiber reinforced polymer (FRP) composite bar (SFCP) using the hand-mode technique. The results of this work showed that the yield stress and tensile strength of SFCB are less than for conventional steel by 4%. While the ratio of bonding strength of SFCB and the bond strength of the steel bar was 0.86, this means that SFCB had low bonding strength compared to normal steel with about 14%.

2. OBJECTIVES OF STUDY

The objective of this investigation is to study the effect of inter-critical temperatures on the microstructural phases and mechanical properties of AISI 1018 low carbon steel such as microhardness, yield strength, tensile strength and wear behavior.

3. EXPERIMENTAL DETAILS

Fig. 1. shows the diagram for the experimental procedures.

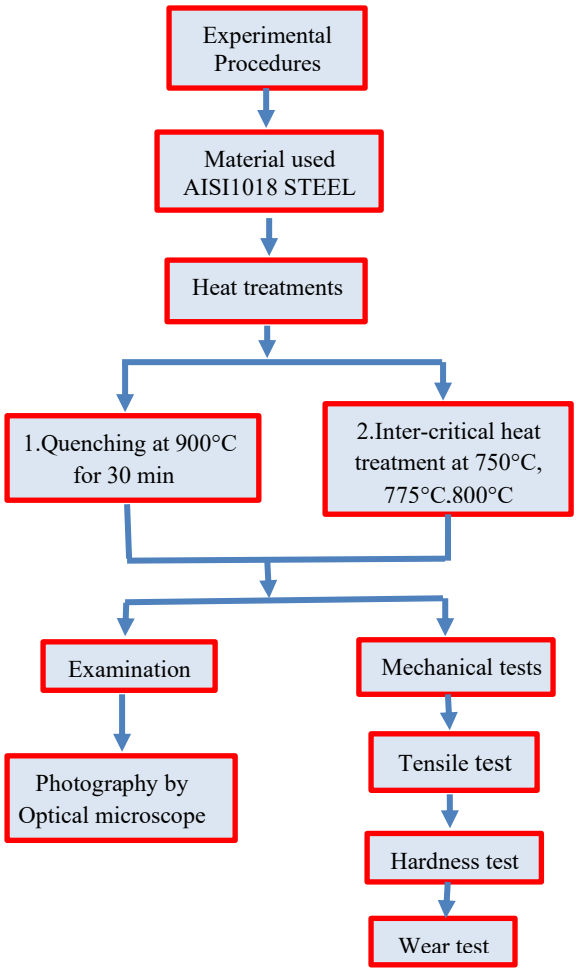

Fig. 1 Diagram for the experimental procedures

3.1. Materials used

The steel used was AISI 1018 alloy steel in bar form. Table 1. shows the values of mechanical characteristics for AISI 1018 while Table 2. shows the weight percentages of each element for the same alloy. Table 3. Shows the number of samples used in the work

Table 1: Mechanical behavior of low carbon steel (Salman, K. D. 2019)

Tensile Strength (MPa)	Yield Strength (MPa)	Vickers Hardness (HV)	Modulus of Elasticity (GPa)	Poisson's Ratio	Elongation (%)
439	369	130	204	0.289	14.9

Table 2: weight percentages of each element for AISI 1018 steel (Salman, K. D. 2019)

C	Si	Mn	P	S
0.121	0.0004	0.440	0.0004	0.027
Cr	Mo	Ni	Al	Co
0.0089	0.0009	0.012	0.0049	0.0009
Cu	Nb	Ti	V	W
0.0133	0.0009	0.00049	0.001	0.0050
Ta	Sn	Zr	Zn	B
0.0082	0.001	0.0054	0.0036	0.0015
As	Pb	Se	Sb	Fe
0.0155	0.001	0.001	0.0071	Remain

Table 3: number of samples used in the work

Number of Samples	Examinations and Testes
4	Photography by Optical Microscope
4	Hardness test
4	Tensile test
4	Wear test

3.2. Heat treatments

Conventional heat treatments are used to produce a special microstructure according to a specific application. So far, the usage of heat treatments on steel alloys is an extremely common practice. Conventional heat treatments of steel alloys are classified as annealing heat treatment, normalizing heat treatment, quenching heat treatment and tempering heat treatment. These treatments are effective in improving the mechanical properties depending on their conditions. In this work, two heat treatments were performed; the first is the conventional heat treatment and the second is the inter-critical heat treatment as follows:

3.2.1. The first heat treatment:

The first heat treatment is the conventional heat treatment. This treatment was performed by heating the samples at 900°C in an electrical furnace for 30 min and then quenched in salt water. In this work, AC1 and AC3 were obtained to be 740°C and 860°C, respectively.

3.2.2. The second heat treatment:

The second heat treatment is the inter-critical heat treatment, this treatment was introduced for

the conventional heat treatment: This treatment was done in the (α+γ) region for the temperatures used in this investigation; 750°C, 775°C and 800°C and then quenched in salt water to room temperature. Fig. 2. illustrates the inter-critical heat treatment.

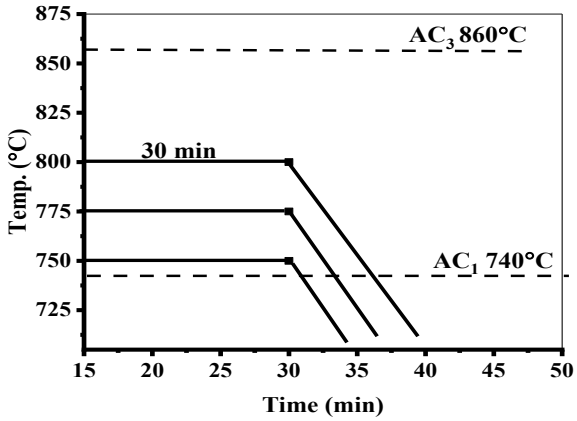

Fig. 2. The inter-critical heat treatment

Afterward, the samples were prepared by grinding using grinding papers with different sizes (180µm, 320µm, 500µm and 1000µm) followed by a polishing process and then the samples were etched by nital solution (2% HNO_3+ 98% alcohol).

3.3. Mechanical testing's

3.3.1. Hardness testing

The dimensions of hardness testing are 1.5 cm in height and 1cm in diameter. Hardness testing was performed using Vickers hardness apparatus with an applied load of 10 Kgf for 15 sec. Many readings were recorded for each sample and then the mean value of hardness was calculated. Hardness testing was done according to (ASTM E-384).

3.3.2. Tensile testing

The tensile testing was done according to (ASTM) (Jaiganesh, V., et. al 2018) using the tensile testing machine type Instron-8516. The velocity of the moving part was constant at 1mm/min. Each of the values of true stress and true strain has been measured from experiments to define the exponent of strain hardening (n) and the plasticity constant (k). Fig. 3. shows the schematic of the tensile sample (Jaiganesh, V., et. al 2018).

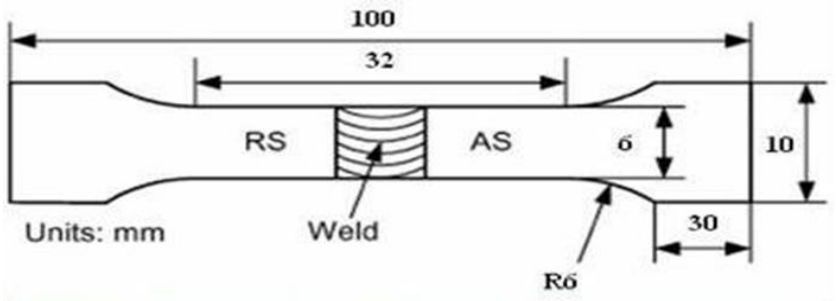

Fig. 3. Schematic diagram of a tensile sample according to (ASTM) (14)

3.3.3. Wear testing

Wear testing was performed using a pin-on-disc machine according to ASTM G-99. Wear testing was done by changing the loads to 5, 10, 15, 20 and 25N for a constant period of 20 min. The dimensions of the samples for dry sliding wear testing were 1cm for the diameter and 3 cm for the length. The wear rate is measured using the following equation (Jiaad, S. M., et. al 2022).

$$\text{Rate of wear} = \frac{\Delta w}{S.D} \quad \text{gm/cm} \tag{1}$$

$$\text{Changing for weight } (\Delta w) = w_1 - w_2 \text{ (gm)} \tag{2}$$

Changing for weight (Δw): represent the changing of weight before and after wear testing.

$$S.D = 2\pi \text{ r n t (cm)} \tag{3}$$

S.D: the sliding distance

Where:

r: the rotating radius of pin-on-disc

n: the rotating speed (500 rpm)

t: testing time (min)

3.4. Microstructural examination

The microstructure features were examined by the FESEM apparatus to estimate the phases of all samples before and after heat treatment.

4. THE OBTAINED RESULTS AND DISCUSSIONS

4.1. Microstructural interpretation

The optical microscopy images of the samples treated by inter-critical heating are revealed in Fig. 4. The first sample (as-received) obviously shows the microstructure containing ferrite phase (white) and pearlite phase (dark). While images of all treated samples show ferrite phase (white) and martensite phase (dark). Increasing in inter-critical heat treatment temperature creates a high volume percent of martensite phase Vm.%. The percent of martensite created in each sample could be interpreted with the lever rule in the α+γ region. Increasing the temperature of heat treatment in the α+γ region creates a higher austenite fraction. The created austenite transforms to martensite by quenching in salt water; hence the percent of the martensite phase for the sample is increased. The percent of martensite phase (Vm.%) was calculated using a special technique (point-count) according to the (ASTM E-562) standard. The values of Vm. % for all inter-critical heat treatment temperatures are listed in Table 4.

Table 4. Volume fractions of martensite for all temperatures.

Metal-alloy	Inter-critical temperature (°C)	Volume fraction of martensite (Vm.%)
AISI 1018 Steel	750	36
	775	61
	800	70

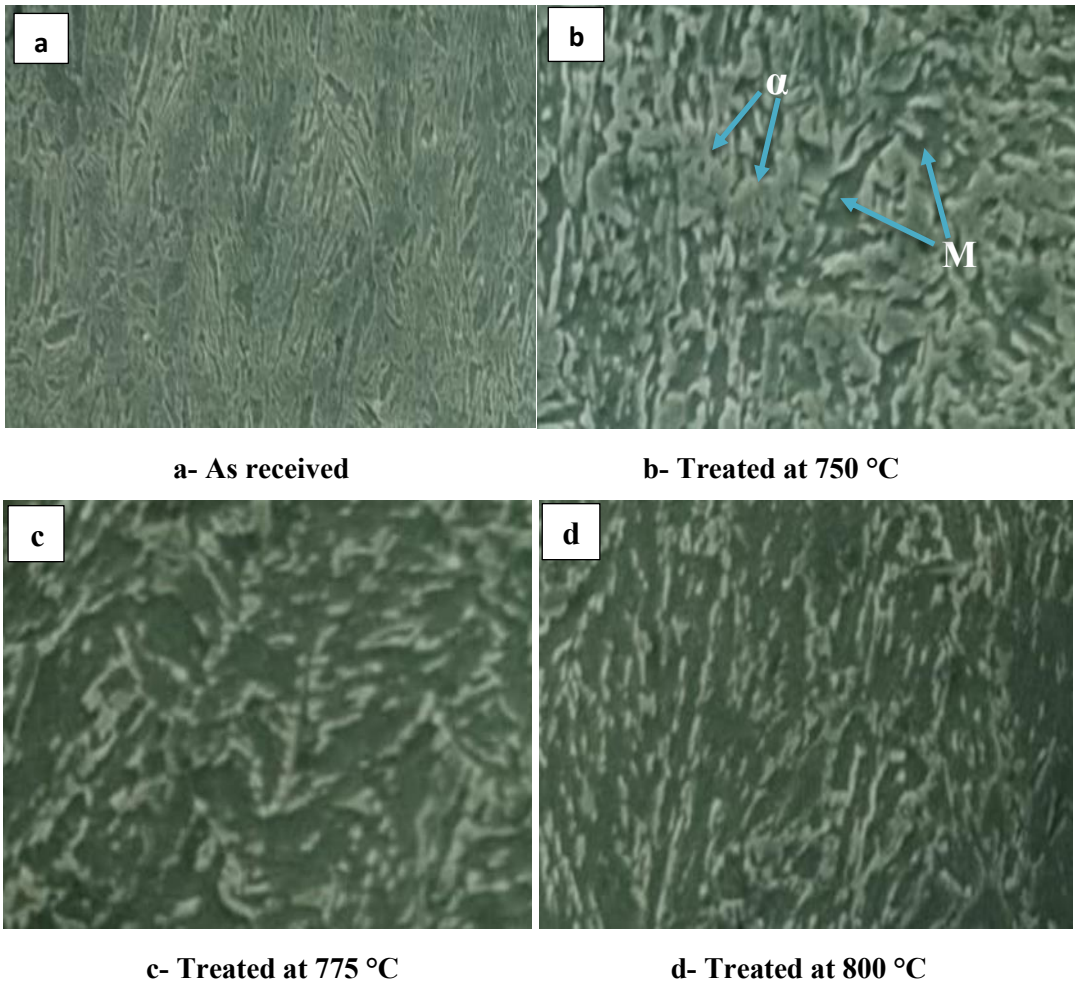

a- As received **b- Treated at 750 °C**

c- Treated at 775 °C **d- Treated at 800 °C**

Fig.4 Optical microscopy images of all treated specimens show ferrite phase (white) and martensite phase (dark)

Fig. 5. represents the topographic surfaces; it is clear that the presence of abrasive grooves. The resistance to the abrasion wear on the worn surfaces is clear to the work hardening. The wear rate of the sample as-received is more than the samples treated by heating at different temperatures. This is owing to the abrasive wear by the pearlite phase being lower than the abrasive wear by the martensite phase. Moreover, the increment of the martensite amount decreases the abrasive wear.

4.2. Hardness results

Fig. 6. illustrates the relationship of Vickers hardness versus Vm.%. The microhardness of the ferrite phase is constant for all inter-critical heat treatment temperatures. It is worth noticing that the carbon percent in ferrite and martensite is directly affected on mechanical properties. The microhardness of ferrite is constant owing to the solubility limit of carbon element in ferrite which is about 0.015 wt.%. The lower hardness value was found for the as-received samples (131 HV). While, the hardness of the inter-critical heat treat samples increases with increasing the heat-treated temperatures owing to the formation of the martensite phase.

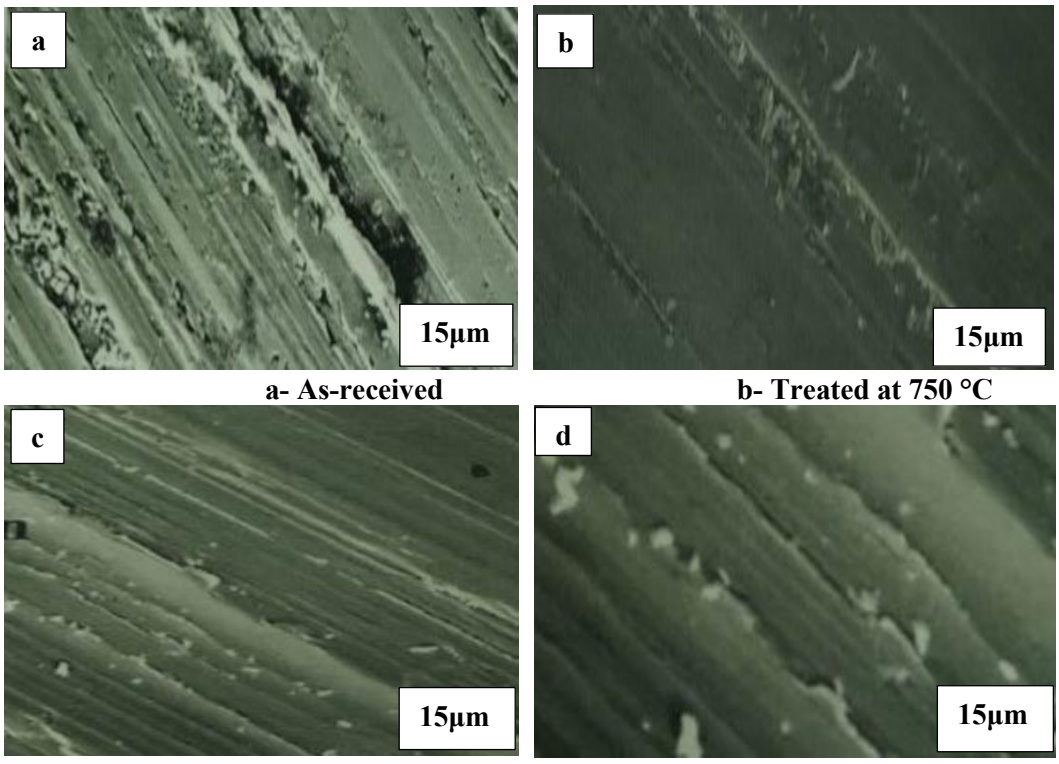

Fig. 5. Surface topography for the samples used in this study

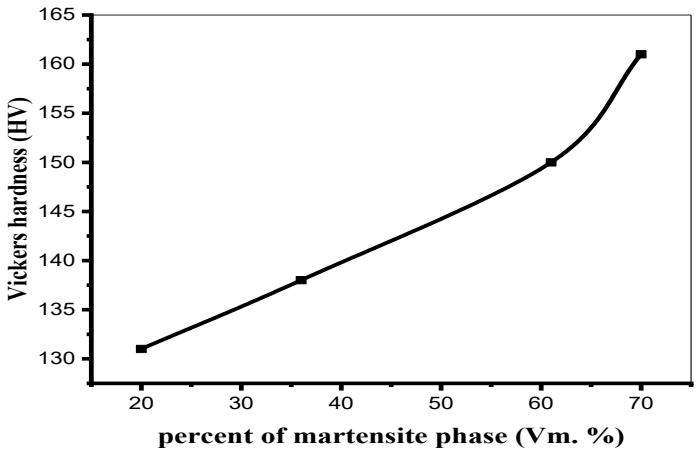

Fig. 6 Vickers hardness versus the percent of martensite (Vm. %)

4.3. Tensile results

Fig. 7. shows the relationships of yielding stress and tensile stress versus the volume fraction of martensite. The yielding strength and tensile strength were increased with increasing inter-critical heat treatment temperatures compared with the yielding stress and tension stress of the received sample. The increment of each yielding stress and tension stress is owing to the created martensite phase from the austenite phase through inter-critical heating treatments. The yield strength is linearly increased with increasing Vm. %, and on the other side the tensile strength increased with the increment of the percent of the martensite phase till to 50 %.

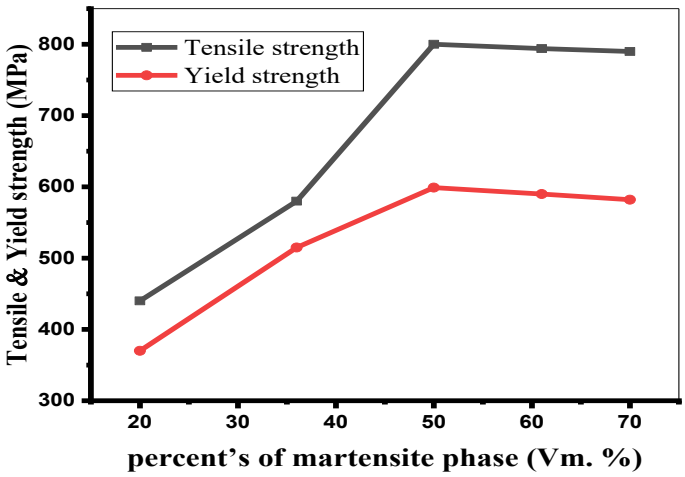

Fig. 7 The relationships between yielding strength and tensile strength versus the percent of martensite phase

On the other hand, plastic deformation was created owing to the changing of the austenite phase to the martensite phase during inter-critical heat treatment. The plastic deformation created at the grain boundary of ferrite and then produced the movement of dislocation at the interfaces of ferrite and martensite. Moreover, the increment of tensile strength is attributed to the increment of carbon percent into the martensite phase. While the reduction of tension strength for a higher volume fraction of martensite (more than 50 Vm. %) is owing to minimizing carbon present in the martensite phase.

4.4. Work hardening

Work hardening of many alloys can be discussed using a flow stress equation named the Hollomon equation (Davari, Mohammad, et. al 2017):

$$\sigma = k\,\varepsilon^{n} \qquad (4)$$

where:

k: coefficient of strength

n: exponent of strain hardening

k and n can be obtained from the relationship ln σ- ln Ɛ. The higher value of (n) means a higher work hardening and higher plastic deformation. The slope of the linear relationship (ln σ- ln Ɛ) gives the exponent of work hardening (n). For the samples with the values of volume fraction of martensite lower than 50 Vm. %, while the work hardening obtained at the single stage, and for the value of martensite volume fraction more than 50 Vm. %, the value work hardening obtained at the second stage. Fig.8. shows the relationships of lnσ and lnƐ for the samples treated by different inter-critical temperatures for the present steel with various amounts of martensite.

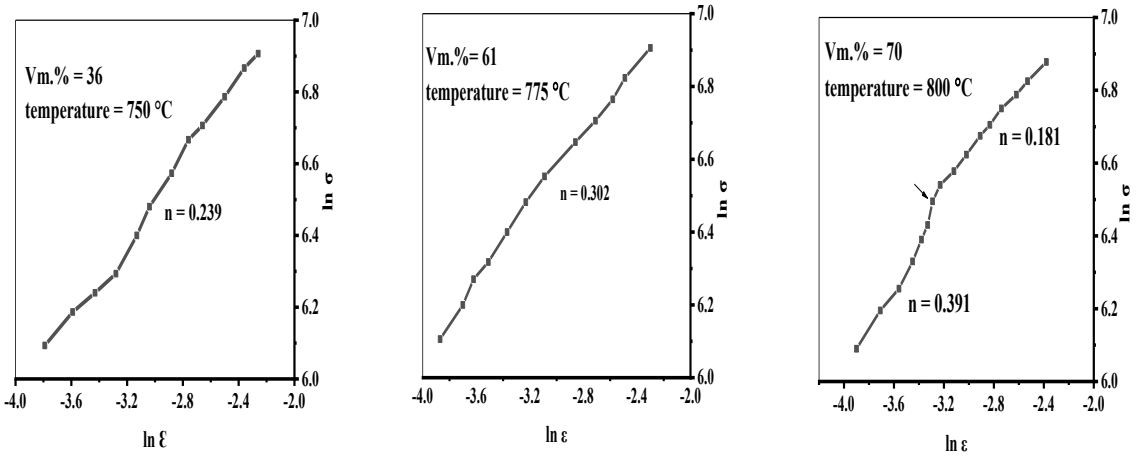

Fig.8 The relationships between ln σ and ln Ɛ for the samples treated by different inter-critical temperatures

4.5. Wear behavior results

Fig. 9. describes the relationships of wear rate versus applied load for all the samples before and after inter-critical heat treatments of dual-phase steel. It is obvious that the increment of the applied load causes an increment in wear rate for the samples used in this investigation.

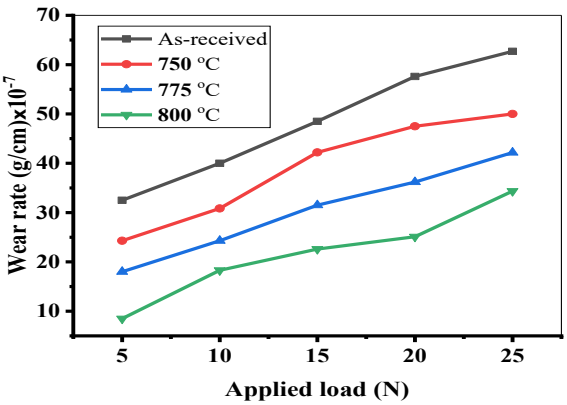

Fig. 9 The wear rate versus applied load for the samples before and after inter-critical heat treatments

Increasing the inter-critical temperature leads to decrease wear rate, it is owing to the change of austenite phase to martensite phase which in turn creates strain hardening. Increasing the heating temperature creates a higher concentration of the martensite phase which is responsible for the decrease in wear rate and then improves the wear properties of the present steel used in this work. Fig.4. represents the topographic surfaces, it is clear that the presence of abrasive grooves. The resistance to the abrasion wear on the worn surfaces is clear to the work hardening. The wear rate of the sample as-received is more than the samples treated by heating at different temperatures. This is owing to the abrasive wear by the pearlite phase being lower than the abrasive wear by the martensite phase. Moreover, the increment of the martensite amount decreases the abrasive wear.

5. CONCLUSIONS

In the present study, the AISI 1018 steel with various amounts of martensite phase was prepared using inter-critical heat treatment. The results showed the following inclusions:

1. The increase of inter-critical heat temperature increases the amount of martensite phase.
2. The amount of martensite equal to 50 Vm. % (ferrite percent equal to martensite percent) exhibits the preferred mechanical properties.
3. The increase in inter-critical heat temperature increases the yielding stress from 370 MPa to 599 MPa, while the tensile strength increases from 440 MPa to 800 MPa and the hardness increases from 131(HV) to 162(HV).
4. The work hardening results showed that the work hardening exponent (n) increases with the increment of inter-critical heat treatment temperature.
5. Single stage work hardening is obtained for the sample containing less than 50 Vm % of martensite. While the double stage work hardening is obtained for the sample containing more than 50 Vm % of martensite.
6. Wear tests showed that the improvement of wear rate was a result of forming the martensite phase. The surface topography for the as-received sample showed that deeper groove, while for the treated samples soft grooves were created.

6. REFERENCES

Davari, Mohammad, and Mehdi Mansouri Hasan Abadi. (2017) "Investigation of intercritical heat treatment temperature effect on microstructure and mechanical properties of dual phase (DP) steel." Metallurgical and Materials Engineering 23.2: 143-152.

Deng, Y., Di, H., & Misra, R. D. K. (2019). Microstructure–mechanical property relationship in hot-rolled high-Al-low-Si dual-phase steel. Ironmaking & Steelmaking, 46(2), 169-175.

Ebrahimian, A., & Banadkouki, S. G. (2017). Mutual mechanical effects of ferrite and martensite in a low alloy ferrite-martensite dual phase steel. Journal of Alloys and Compounds, 708, 43-54.

Hertzberg, R. W., Vinci, R. P., & Hertzberg, J. L. (2020). Deformation and fracture mechanics of engineering materials. John Wiley & Sons.

Hug, E., Martinez, M., & Chottin, J. (2015). Temperature and stress state influence on void evolution in a high-strength dual-phase steel. Materials Science and Engineering: A, 626, 286-295.

Hug, E., Martinez, M., & Chottin, J. (2016). Thermomechanical properties of high martensitic dual-phase steels related to dislocation structures and void damage evolution. Advances in Materials and Processing Technologies, 2(2), 339-347.

Hussein, A., Abbas, L., & Hassan, W. (2019). Optimization of steel hardness using nanofluids quenchants. Kufa Journal of Engineering, 10(1), 29-43.

Jaiganesh, V., Srinivasan, D., & Sevvel, P. (2018). Optimization of process parameters on friction stir welding of 2014 aluminum alloy plates. International Journal of Engineering & Technology, 7(1.1), 9-11.

Jiaad, S. M., Salman, K. D., & Hussein, A. (2022, December). Evaluation of the microstructure and mechanical properties of hybrid aluminium composite reinforced by Fe3O4 and Ni nano particles. In AIP Conference Proceedings (Vol. 2415, No. 1). AIP Publishing.

Jiang, J., Wu, H., Liang, J., & Tang, D. (2013). Microstructural characterization and impact toughness of a jackup rig rack steel treated by intercritical heat treatment. Materials Science and Engineering: A, 587, 359-364.

Lai, Q., Bouaziz, O., Gouné, M., Brassart, L., Verdier, M., Parry, G., ... & Pardoen, T. (2015). Damage and fracture of dual-phase steels: Influence of martensite volume fraction. Materials Science and Engineering: A, 646, 322-331.

Namdev, A., Telang, A., Purohit, R., & Kumar, A. (2022). The effect of inter critical heat treatment on mechanical and wear properties of AISI 1015 steel. Advances in Materials and Processing Technologies, 8(sup2), 434-444.

Pandre, S., Takalkar, P., Morchhale, A., Kotkunde, N., & Singh, S. K. (2020). Prediction capability of anisotropic yielding behaviour for DP590 steel at elevated temperatures. Advances in Materials and Processing Technologies, 6(2), 396-404.

Papa Rao, M., Subramanya Sarma, V., & Sankaran, S. (2014). Processing of bimodal grain-sized ultrafine-grained dual phase microalloyed V-Nb steel with 1370 MPa strength and 16 pct uniform elongation through warm rolling and intercritical annealing. Metallurgical and Materials Transactions A, 45, 5313-5317.

Pervaiz, S., Deiab, I., & Kishawy, H. (2016). A finite element based energy consumption analysis for machining AISI 1045 carbon steel using uncoated carbide tool. Advances in Materials and Processing Technologies, 2(1), 83-92.

Salman, K. D. (2019, August). Microstructure and Mechanical Properties of Cold Rolled AISI 1018 Low Carbon Steel. In IOP Conference Series: Materials Science and Engineering (Vol. 551, No. 1, p. 012007). IOP Publishing.

Shukla, N., Roy, H., & Show, B. K. (2016). Effect of prior austempering heat treatment on the microstructure, mechanical properties and high-stress abrasive wear behaviour of a 0· 33% C dual-phase steel. Canadian Metallurgical Quarterly, 55(1), 13-22.

Shukur, S. A., & Alkhudery, H. H. A. H. H. (2023). EXPERIMENTAL ASSESSMENT OF THE MECHANICAL PROPERTIES OF STEEL-FIBER COMPOSITE BAR (SFCB) REINFORCEMENT. Kufa Journal of Engineering, 14(1), 50-66.